J Solid State Electrochem (1998) 2: 2–6

ORIGINAL PAPER

Miriam Gálová · Renata Oriňáková · Ladislav Lux

Distribution of charge in the process of coating Fe powder by electrolysis in a fluidized bed

Received: 5 May 1997 / Accepted: 30 June 1997

Abstract Theoretical calculations of the amount of Ni that is applied electrolytically in the form of a coating on Fe powder particles in a fluidized bed are based upon the assumption of distribution of charge between the surface of the solid cathode and the powder particles present in the working volume of the electrolyte. The experimentally measured data show good agreement with theory. The efficiency of the coating process is rather low because of inhibition of the process by hydroxocomplexes formed in the course of electrolysis. The inhibition effect becomes more significant in the case of high suspension density, small powder particles, high current density, and prolonged time of electrolysis.

Key words Fluidized bed electrolysis · Fe powder coating · Charge distribution

Introduction

The process of electrolytical coating of powder particles could achieve great importance in powder metallurgy. In order to modify base metal material, several procedures can be adopted. Electrochemical deposition of metal plating on the powder is one of the processes that give the best homogeneity of the product. Experimentally, this process was extensively developed and optimized for electrolytic coating of nickel on the surface of Fe powder particles [1]. One partial theoretical problem, namely the change in the solid electrode surface as a consequence of metallic particles touching it, was solved for various suspension densities and mean particle sizes by means of a model suggested in [2]. A type of fluidized bed electrode realized by pouring the solid Fe powder particles into the electrolyte under intensive circular stirring was used in these experiments as well as in the present work.

The theory of fluidized bed electrodes has been treated by many authors. Fleischmann and Oldfield were the first to introduce the mechanism of elastic collisions in charge transfer in the operation of fluidized bed electrodes [3, 4]. Here, it is assumed that the double layers of the particles in the bed are charged when they contact the solid electrode or other charged particles. A different charge transfer mechanism called the conductive mechanism was described by Sabacky and Evans [5] and Plimley and Wright [6]: particles in the fluidized bed form aggregates and chains which contact either the electrode or other chains. Charges pass through the chains by electronic conduction. A chain exists for a short period of time and then is destroyed and reformed as another particle chain. Yen and Yao [7, 8], describing the application of a fluidized bed electrode for metal recovery from dilute electrolyte solutions, made an analysis of the bipolar behavior of a solid single sphere in an electric field in the fluidized bed, and suggested a mathematical model for two surface conditions: linear polarized kinetics and Butler-Volmer kinetics. Gabrieli and coworkers [9, 10] based their model of the fluidized bed electrode in a dynamic regime upon earlier work by Newman and Tobias [11] presenting a porous electrode model. The authors used the impedance technique for describing a porous electrode varying randomly with time, with electro-inactive as well as electro-active particles in the bed.

In the present work an attempt has been made to expand the above-mentioned model [2] and to analyze the distribution of charge passing through the fluidized bed electrode between the solid cathode and powder particles on one side and between the required and side reactions on the other. The suspension density, together with the size of the bed-forming particles, are two of the

M. Gálová (✉) · R. Oriňáková
Department of Physical and Analytical Chemistry,
P.J. Šafárik University, 04154 Košice, Slovakia
Tel.: +42-195-6228114; e-mail: mgalova@kosice.upjs.sk

L. Lux
Department of Chemistry, Technical University,
04200 Košice, Slovakia
Tel.: +42-195-6330298; e-mail: luxlad@ccsun.tuke.sk

most important parameters influencing the distribution of charge.

Theoretical

The distribution of charge between solid cathode and powder particles is based on the model presented in detail in [2]. The concept of "working volume", which was introduced in that paper, refers to the volume of the electrolyte suspension attached to the electrode in which the powder particles are in direct contact with the electrode. The working fraction of the electrolyte suspension can be expressed in terms of the cell geometry by the dimensionless parameter K:

$$K = \frac{s^2 \arcsin\,(s/d)}{d^2 \pi} \tag{1}$$

where s is the width of the solid cathode and d is the diameter of the cathodic compartment. The working volume (W_V) of the electrolyte can be calculated according to Eq. 2a, while the mass of the powder particles in it (W_m) is given by Eq. 2b:

$$W_v = K\ V_{CATH} \qquad (\text{in cm}^3) \tag{2a}$$

$$W_m = K\ m_{POW} \qquad (\text{in g}) \tag{2b}$$

where V_{CATH} is the total volume of the electrolyte in the cathodic compartment and m_{POW} is the total amount of powder particles added into the cathodic compartment (in g).

Calculation of the specific surface area S_A of the powder particles was based on the assumption of their spherical shape, using the respective mean radius r of the given granulometric class [2]:

$$S_A = \frac{3}{r\,\rho} \quad (\text{in cm}^2/\text{g}) \tag{3}$$

where ρ is the specific mass of the powder substance (for Fe powder $\rho = 7.88$ g/cm^3).

The calculated specific surface areas for various particle sizes represented by mean diameters d_m of the powder particle fraction are summarized in the second column of Table 1. The third column of Table 1 shows the total surface area of the powder present in the working volume of the electrolyte suspension S_P (for one value of suspension density). It is calculated as follows:

$$S_P = m_{POW}\ S_A\ K \qquad (\text{in cm}^2) \tag{4}$$

The values for other suspension densities used were calculated similarly. The last column of Table 1 represents the fraction of the electrode surface formed by powder particles S_E:

$$S_E = \frac{S_P}{S_{CATH} + S_P} \times 100\ (\%) \tag{5}$$

S_{CATH} is the geometrical surface area of the solid cathode (in cm^2).

In the following considerations it is assumed that the charge is distributed uniformly on the whole surface area participating in the electrolysis. Consequently, the amount of metal coating is distributed in the same ratio as the charge. The theoretical amount of charge on the powder particles Q_{POW}(theor) is then calculated in the same way as the fraction of the surface area of powder particles in W_V:

$$Q_{POW}(\text{theor}) = \frac{S_P}{S_{CATH} + S_P} \times 100\ (\%) \tag{6}$$

The calculated results of Q_{POW}(theor) for different suspension densities and particle size fractions are presented in Fig. 1. Based on the above calculated distribution of the charge, the theoretical amount as well as the theoretical percentage of metal coating on powder particles may be calculated according to the Eqs. 7a and 7b:

$$m_{Me}(\text{theor}) = \frac{Q_{POW}(\text{theor})\ I\ t\ M_{Me}}{2\ F\ 100} \tag{7a}$$

Table 1 Theoretical fraction of the powder surface participating in the electrolysis. Voidage factor expressed as $(1 - \varepsilon)\ 10^3 = 8.39$; surface area of the solid cathode: 15.74 cm^2; d_m, mean particle size; S_A, calculated specific surface area of the powder present in the working volume; S_P, total surface area of the powder present in the working volume; S_E, portion of the electrode surface formed by powder particles

d_m mm	S_A cm^2 g^{-1}	S_P cm^2	S_E %
0.02	380.7	141.362	89.99
0.05	152.3	56.65	78.26
0.08	95.2	35.41	69.23
0.1125	67.7	25.18	61.54
0.1425	53.3	19.86	55.79

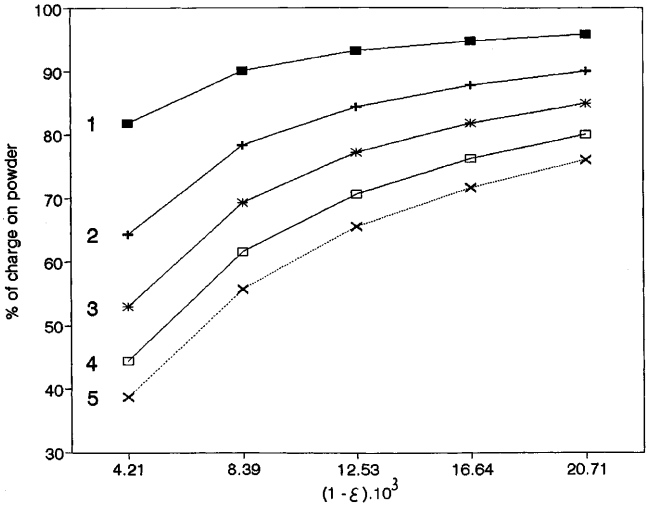

Fig. 1 Theoretical charge distribution between powder particles and solid cathode for various suspension densities. Mean particle size: curve 1, 20 μm; curve 2, 50 μm; curve 3, 80 μm; curve 4, 112.5 μm; curve 5, 142.5 μm

I and t represent the current passing through the cell and the electrolysis time, respectively, M_{Me} is the molar mass of the metal, and F is the Faraday constant.

$$\%_{Me}(\text{theor}) = \frac{m_{Me}(\text{theor})}{m_{Me}(\text{theor}) + m_{POW}} \times 100\ (\%) \qquad (7b)$$

The calculated values of % of Ni coating on Fe powder particles of the particle size class characterized by the mean diameter 50 μm are shown in Fig. 2. The electrolysis time was 3600 s, and the total current passing 1 A and 3 A, respectively.

Experimental

The process studied here was the electrolytic coating of Fe powder particles by nickel in an electrolyte of pH 2 containing 1.2 mol dm^{-3} $NiSO_4$, 0.6 mol dm^{-3} NaCl, and 0.6 mol dm^{-3} H_3BO_3. Fe powder particles with mean linear dimensions 20, 50, 80, 112.5, and 142.5 μm were used. Prior to electrolysis, the powder was activated by chemical treatment with a reducing agent (a 10% solution of hydroxylamine hydrochloride), rinsed with methanol and dried. The electrolytic cell consisted of a cathodic compartment (150 ml in volume) separated from the anodic compartment by a diaphragm (textile net with mesh size of about 0.04 mm). The compartments were separately stirred. A solid stainless steel plate of geometric surface 15.74 cm^2 was used as the current feeder. The counter electrode placed opposite the current feeder in the anodic compartment was made from pure nickel. The movement of the stirrer in the cathodic compartment was electronically controlled and kept constant within ± 10 rpm. The suspension density values were expressed in terms of voidage factor $(1 - \varepsilon) = V_p/(V_p + V_e)$; V_p and V_e are the volumes of solid powder particles and liquid electrolyte, respectively [12]. In the experimental apparatus used in the present work, the calculated dimensionless parameter K had the value 0.0372. It represented a working volume of $W_v = 5.58\,cm^3$. Experimental values of the mass of Ni and % $Ni_{(exp)}$ on powder were obtained by AAS and gravimetric analyses. Efficiency of the process on the powder particles η_{POW} was then calculated by either of the following equations:

$$\eta_{POW} = \frac{Q_{POW}(\text{exp})}{Q_{POW}(\text{theor})} \times 100\ (\%) \qquad (8a)$$

$$\eta_{POW} = \frac{m_{Ni}(\text{exp})}{m_{Ni}(\text{theor})} \times 100\ (\%) \qquad (8b)$$

Results and discussion

Figure 2 presents the theoretically calculated and experimentally found percentages of Ni on Fe powder particles. It is evident that in all cases the shapes of the theoretical and experimental curves are identical: with increasing suspension density the quantity of the powder and therefore the surface area to be coated is larger, and consequently the percentage of Ni coating on the powder for the same charge passed is lower. The differences between theoretical and experimentally measured values are included in the above defined quantity η_{pow} (see Eqs. 8a and 8b) and shown in Fig. 3. From the curves in Fig. 3 it is clearly seen that the efficiency of the process of coating the powder decreases with increase of both the suspension density and the current density. It is well known in plating practice that metal deposition from acidic baths is accompanied by hydrogen evolution. With increase in the current density, the hydrogen evolution process is favored and thus the efficiency of the process decreases. Evidently, the hydrogen evolution effect takes place also on the powder particles and contributes to the decrease in η_{pow}. As a result of increasing suspension density the surface area of the electrode increases and thus the current density decreases. With hydrogen evolution as the only side reaction the increase in the powder coating efficiency η_{pow} with increasing suspension density would therefore be

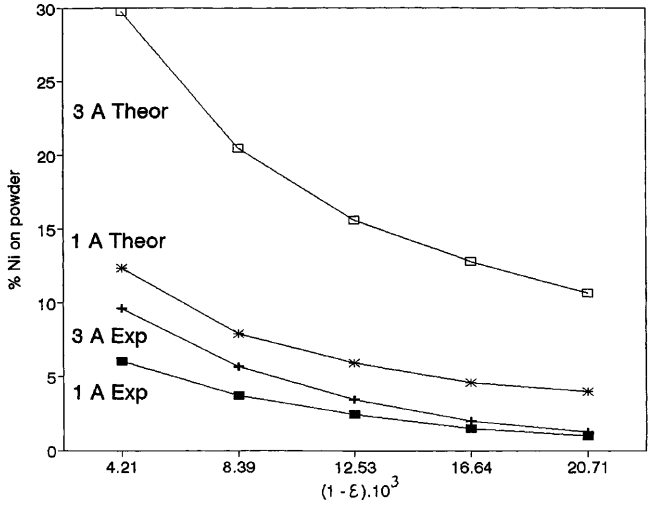

Fig. 2 Comparison of theoretical and experimentally determined Ni content in % on Fe powder particles with increasing suspension density (1 - ε), for 1-A and 3-A electrolysis current. Mean particle size 50 μm

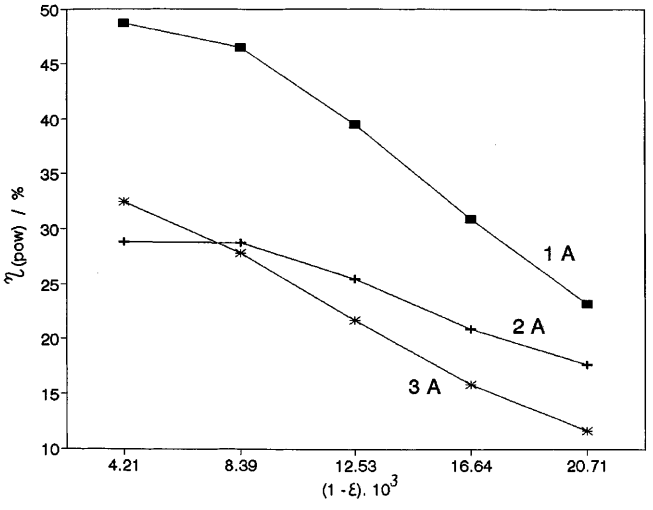

Fig. 3 Efficiency of the electrolytical process of coating the powder particles. Mean particle size 50 μm. Electrolysis current 1 A, 2 A, and 3 A

expected. This however is not the case, as shown in Fig. 3. This fact will be discussed later in the text.

In order to verify the charge distribution model, the absolute amount of Ni deposited on Fe powder particles, which is directly proportional to the charge on them, should be considered. Figures 4 and 5 show the comparison of theoretically calculated and experimentally observed values of deposited Ni on the Fe powder in weight units. Figures 4 and 5 differ in the size of the coated particles. For the larger size fraction, characterized by a mean particle size of 112.5 μm (Fig. 4), the shapes of the theoretical and experimental curves for a current of 1 A are again identical. When the current is 3 A, the rise in the experimental curve is much slower than that of the theoretical one. At higher suspension densities a small fall can even be observed in the experimental curve. The fall that occurs in the experimental curves with the increase in suspension density is much more noticeable in the case of the smaller size fraction, characterized by the mean particle size 50 μm, as can be seen in Fig. 5. The results presented point to the fact that the hydrogen evolution reaction is not the dominant side reaction causing the decrease of experimental amounts of Ni deposited on Fe particles with increasing suspension density.

In order to explain the generally observed differences in the theoretical and experimentally observed amount of Ni on the powder, the following points should be considered. As a consequence of hydrogen evolution the pH value in the bulk of the electrolyte increases in the course of electrolysis, more so in the vicinity of the cathode. This leads to the formation of various insoluble nickel hydroxocomplexes [13–17]. In addition to this, the Fe powder particles undergo partial dissolution, and consequently, with increase of pH value, insoluble hydroxocomplexes of iron are also formed. Both Fe and Ni hydroxocomplexes can be adsorbed on the powder particles and inhibit further Ni deposition. Our earlier experiments proved [18] that in the course of the electrolytic process the amount of Ni deposited on the particles actually decreases with time and eventually can be completely stopped due to the competitive adsorption of insoluble hydroxocomplexes on the surface of the powder. An example of the time dependence of the amount of Ni coated during the electrolysis is shown by curve 3 in Fig. 6. Curve 1 in this figure shows the theoretical amount of Ni coated on the particles calculated

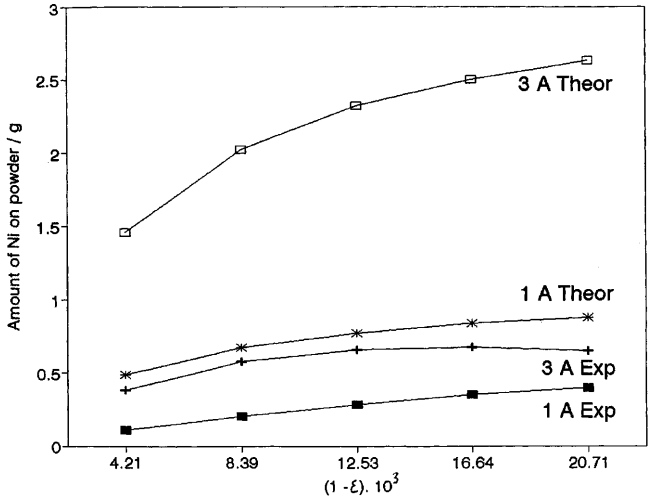

Fig. 4 Comparison of theoretical and experimentally determined amount of Ni in weight units on Fe powder particles with increasing suspension density (1 - ε), for 1-A and 3-A electrolysis current. Mean particle size 112.5 μm

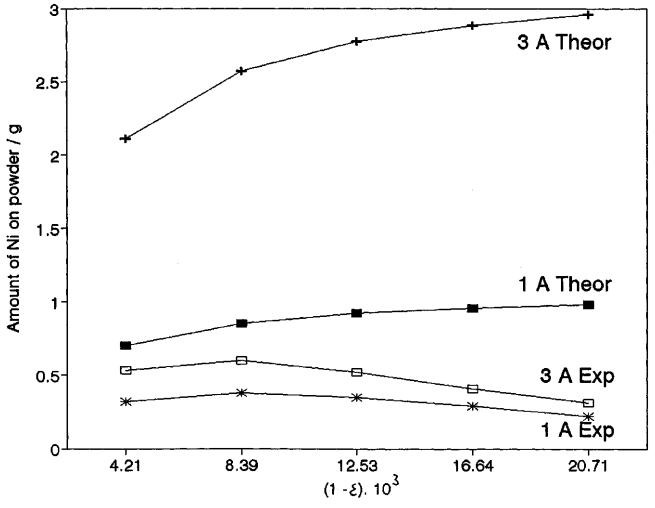

Fig. 5 Comparison of theoretical and experimentally determined amount of Ni in weight units on Fe powder particles with increasing suspension density (1 - ε), for 1-A and 3-A electrolysis current. Mean particle size 50 μm

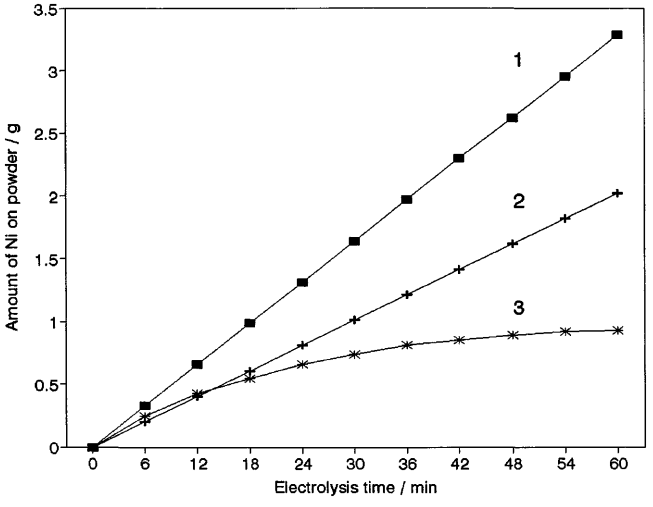

Fig. 6 Theoretical and experimentally determined amount of Ni deposited on powder in the course of electrolysis. Mean particle size: 112.5 μm, suspension density $(1 - \varepsilon) \cdot 10^3$, 8.39. Curve 1, theoretical amount of Ni deposited calculated according to Faraday's Law; curve 2, theoretical amount of Ni deposited based on the charge distribution (see Fig. 1); curve 3, experimental data

according to Faraday's law assuming that the whole charge is realized on the particles. Curve 2 is calculated taking into account the distribution of charge between the solid cathode and the powder particles as discussed above (see Fig. 1).

Both the increase in the powder quantity in the electrolyte (the suspension density) and the decrease in particle size lead to the increase in the surface area of the Fe powder, and consequently promote the dissolution of Fe and the formation of an inhibiting adsorbed layer on the powder. Experimental curves for 1 A and 3 A in Fig. 5 prove the influence of increasing suspension density on the formation of the inhibiting layer. Comparison of the above-mentioned curves in Fig. 5 with the experimental curves for 3 A in Fig. 4 prove the influence of the particle size on this effect: in the case of larger particles (Fig. 4) the inhibiting effect occurs at higher suspension densities than in the case of smaller particles (Fig. 5).

In conclusion, it can be stated that the coating of powder particles by metal can be realized in the experimental arrangement described above as far as the electrode reaction itself proceeds on the given metal. It is likely that this holds not only for the chosen system of metals but in general for metal- metal powder electrolysis. The thickness of the metal coating layer on the powder is controlled mainly by the parameters: powder-to-electrolyte ratio, current density, and particle size, as well as other influences.

References

1. Gálová M, Lux L, Dudrová E, Stašková R (1994) Trans Techn Univ Košice No 3/4: 185
2. Lux L, Stašková R, Gálová M (1996) Acta Chim – Models in Chemistry 133: 115
3. Fleischmann M, Oldfield JW (1971) J Electroanal Chem 29: 211
4. Fleischmann M, Oldfield JW (1971) J Electroanal Chem 29: 231
5. Sabacky BJ, Evans JW (1977) Metall Trans 8B: 5
6. Plimley RE, Wright AR (1984) Chem Eng Sci 39: 395
7. Shi-Chern Yen, Ching-Yih Yao (1991) J Electrochem Soc 138: 2344
8. Shi-Chern Yen, Ching-Yih Yao (1991) J Electrochem Soc 138: 2697
9. Gabrielli C, Huet F, Sahar A, Valentin G (1992) J Appl Electrochem 22: 801
10. Gabrielli C, Huet F, Sahar A, Valentin G (1994) J Appl Electrochem 24: 481
11. Newman JS, Tobias CW (1962) J Electrochem Soc 109: 1183
12. Roušar I, Micka K, Kimla A (1986) Electrochemical engineering, vol 2. Academia Praha p 93
13. Grande WC, Talbot JB (1993) J Electrochem Soc 140: 669
14. Grande WC, Talbot JB (1993) J Electrochem Soc 140: 675
15. Saleh MM, Weidner JW, Ateya BG (1995) J Electrochem Soc 142: 4113
16. Saleh MM, Weidner JW, El Anadouli EB, Ateya BG (1995) J Electrochem Soc 142: 4122
17. Arvia AJ, Posadas D (1972) In: Bard AJ (ed) Encyclopedia of the elements (nickel) Dekker, New York, pp 211–421
18. Oriňáková R, Gálová M, Lavrin A, Lux L (1996) In: Proceedings of the Conference on Preparation and Characterization of Particular Substances, Košice, p 72